9, 1197 (1971).
[11]S. N. Jasperson and S. E. Schnatterly, Rev. Sci. Instr. 40, 761 (1969).
[12]See, for instance, M. J. Freiser, IEEE Trans. Magnetics 4, 152 (1968).
[13]See, for instance, V. Rojansky, *Introductory Quantum Mechanics* (Prentice-Hall, Englewood Cliffs, N.J., 1938), Chap. 6.
[14]R. M. Hill, Proc. Roy. Soc. (London) A309, 377 (1969).
[15]See, for instance, R. M. Bozorth, *Ferromagnetism* (Van Nostrand, Princeton, N.J., 1951), Chap. 16.
[16]R. M. Bozorth, *Ferromagnetism* (Van Nostrand, Princeton, N.J., 1951), Chap. 12.
[17]A. H. Morrish, *The Physical Principles of Magnetism* (Wiley, New York, 1965), Chap. 7, Sec. 3.
[18]J. S. Kouvel and J. B. Comly, Phys. Rev. Letters 24, 598 (1970).
[19]M. Fibich and A. Ron, Phys. Rev. Letters 25, 296 (1970).
[20]L. Onsager, J. Am. Chem. Soc. 58, 1486 (1936).
[21]A. H. Morrish, *The Physical Principles of Magnetism* (Wiley, New York, 1965), Chap. 7, Sec. 3, p. 362.

PHYSICAL REVIEW B VOLUME 5, NUMBER 9 1 MAY 1972

The $AuAl_2$-$AuGa_2$-$AuIn_2$ Problem: Knight Shifts and Relaxation Times in Their Pseudobinary Alloys

G. C. Carter, I. D. Weisman, L. H. Bennett
Institute for Materials Research, National Bureau of Standards, Gaithersburg, Maryland 20760
and
R. E. Watson*
Brookhaven National Laboratory,† Upton, New York 11973
(Received 25 June 1971)

The nuclear-magnetic-resonance (NMR) and susceptibility behavior of the intermetallic compound $AuGa_2$ differs anomalously from the isoelectric and isostructural compounds $AuIn_2$ and $AuAl_2$. In an effort to test and extend the explanation offered by Jaccarino *et al.* and by Switendick and Narath, spin-lattice relaxation times and Knight shifts have been measured as a function of temperature and composition for the $AuAl_2$-$AuGa_2$, $AuAl_2$-$AuIn_2$, and $AuGa_2$-$AuIn_2$ pseudobinary alloy systems. At high temperature, the solute X (Al, In, Ga) resonance properties are dominated by the host. Satellite resonances are observed with temperature dependences differing from the main resonance. The results are partially explainable on the basis of an average-band model and partially on a local atom model. The role of the Au d bands is discussed. Metallurgical results on alloying are obtained using the NMR data.

I. INTRODUCTION

The three intermetallic compounds, $AuAl_2$, $AuGa_2$, and $AuIn_2$, are at once interesting and confusing. The three, all crystallizing in the fluorite structure, display similarities and dissimilarities which, to date, would seem to be incompatible. The most striking difference[1] among the three is the fact that $AuGa_2$ has a strongly temperature-dependent susceptibility χ and Knight shift $\mathcal{K}$, the latter reversing sign, whereas the other two compounds display temperature independence. Explanation of the $AuGa_2$ data apparently requires a model,[1] henceforth denoted JWWM (after Jaccarino, Wernick, Weger, Menth), involving a very substantial modification with temperature of the band character at the Fermi surface.

Switendick and Narath[2] calculated the electronic band structures of the three compounds. They uncovered a feature of the $AuGa_2$ bands not present in the others, which could lead to a band-repopulation effect, which in turn could explain the Knight-shift behavior but not necessarily the susceptibility. Such an effect, or in fact, any band modification yielding the Knight-shift variation, would be expected to be reflected in the electrical properties of this metal. The thermoelectric power is anomalous.[3] But Hall-effect,[3] resistivity,[3,4] and magnetoresistivity[4] measurements display no anomalous variation with temperature in this compound. These facts are central to the "puzzle" of the AuX_2 compounds.

In an effort to further explore this matter, we have obtained Knight-shift and relaxation-time results at host and impurity-X sites in the dilute pseudobinary alloys formed by the AuX_2 compounds with each other. The results are consistent with the JWWM model. They supply no obvious justification or refutation of the existing band calculation for the $AuGa_2$ behavior, but they add some in-

teresting constraints on the ultimate description of these compounds. The impurity-site behavior, for small impurity concentrations, is generally dominated by the host's properties in all three compounds. This is not necessarily surprising in the light of the Switendick-Narath band results, but contrasts with some other alloy systems where the introduction of a *local* susceptibility is important in order to understand solute-site behavior.[5] Either average-band or local behavior can be used to explain the result that concentrations of 5 at. % Al or 10 at. % In "poison" the $AuGa_2$ matrix, destroying its temperature dependence. On the other hand, there are also some important manifestations of purely local behavior. Two distinct Knight shifts are seen for a particular host species in a given sample in some of the alloys. The temperature behavior of these is surprisingly, and likely to be misleadingly, similar to effects seen for magnetic impurities in alloys such as ^{59}Co in Mo, where the Knight shift for the site with the local moment varies with temperature while the other site does not,[6,7] or such as ^{51}V in Au, where a magnetic and a nonmagnetic site are distinguishable at low temperatures.[8]

II. BACKGROUND

$AuAl_2$ is mauve colored[9] while the other two AuX_2 compounds are metallic in color with some question of a blue tinge. To this group one could also add the isostructural compound $PtGa_2$ which is yellow in color. Optical transitions involving the $5d$ bands have been suggested to account for the colors of the AuX_2 compounds,[10] although the assumption that the d bands are too low lying has led to other explanations.[2,11] In the fluorite $cF12$ structure, the Au atoms sit on a fcc lattice with eight near-neighbor X atoms. Each X-site atom has four Au-atom near neighbors, six X-atom second-nearest neighbors, and twelve X-atom third-nearest neighbors. The lattice constants are somewhat smaller than might be inferred from metallic radii considerations, suggesting the existence of covalent bonding.[9,10,12] We might note that Au in pure Au metal is squeezed and we are inclined[13] to attribute this to strong s-d hybridization rather than to conventional covalency. This attribution would have less justification for the present compounds since the d bands are thought to lie further below the Fermi level, thus reducing their hybridization. The suggestion of strong covalency, the diamagnetism of these compounds, and the fact that they contract upon melting[14] would seem to imply that they should be viewed as similar to semimetals.[10] They are, however, quite good conductors; the room-temperature resistivities of $AuAl_2$ and $AuIn_2$ are approximately five times that of pure Cu while that for $AuGa_2$ is a little greater.

de Haas–van Alphen[15] and high-field galvanomagnetic[4] experiments have been done to ascertain the Fermi surfaces of these compounds. The results were reasonably well accounted for using a common free-electron band structure occupied by seven electrons (one Au and three for each X atom). The $AuGa_2$ data showed no striking differences from the other compounds: On occasion it was different, but equally often $AuGa_2$ and $AuIn_2$ were alike and $AuAl_2$ different. This is typical of these systems: At times it is $AuGa_2$ and at other times it is $AuAl_2$ which looks different from the other two.

Hall-effect and resistivity measurements show no clear distinction between the three materials but the thermoelectric power of $AuGa_2$ goes negative at high temperatures while those of the other two do not.[3] This seems to suggest[3] striking differences in electronic character at the $AuGa_2$ Fermi surface as does the temperature dependence of the Knight shift and susceptibility.[1,2] The difficulty is, of course, that almost no other data display such effects.

Jaccarino and co-workers studied[1,16] the X-site Knight shifts and the magnetic susceptibilities in these three and some isostructural Pt compounds. The ^{27}Al and ^{115}In resonance frequencies for $AuAl_2$ and $AuIn_2$ were temperature independent, as were the susceptibilities of these compounds whereas ^{69,71}Ga in $AuGa_2$ shows a substantial temperature variation from $\mathcal{K} \sim -0.1\%$ at low temperatures to $\sim +0.5\%$ at high temperatures. The room-temperature value is similar, considering atomic hyperfine constants, to the shifts obtained for the ^{115}In in $AuIn_2$. The temperature variation in the Ga shift tracks the $AuGa_2$ susceptibility quite faithfully, i.e., it may be described by

$$\chi_{\text{tot}} = \chi(T) + \text{temp-ind terms}, \tag{1}$$

$$\mathcal{K}^{\text{Ga}}_{\text{tot}} = \frac{W^{\text{Ga}}}{N\mu_B} H^{\text{Ga}}_{\text{eff}} \chi(T) + \text{temp-ind terms}, \tag{2}$$

where W^{Ga} and $H^{\text{Ga}}_{\text{eff}}$ are the fractional weight of Ga character and the Ga-site hyperfine constant associated with the band(s) in question. In such a case, one normally[17] attributes $\chi(T)$ to a temperature-dependent band paramagnetism. JWWM pointed out[1] that this could not describe the case here. First, the $H^{\text{Ga}}_{\text{eff}}$ so deduced (setting $W^{\text{Ga}} = 1$) is negative (see Table I) and roughly two orders of magnitude too large[17] to be attributed to such sources of negative hyperfine constants as p-band core polarization. Second, the susceptibility becomes more diamagnetic with increasing temperature (suggesting the disappearance of a paramagnetic term) but relaxation time T_1 results show an increase in s-band character with increasing temperature (indicating the turning on of an s-band paramagnetic term). It thus appears that at least two tempera-

TABLE I. $AuGa_2$ hyperfine fields deduced from various estimates of $\mathcal{K}$ and χ.

Method of estimate	Site	H_{eff}(kOe/μ_B)	Ref.
From low temperature $\mathcal{K}$, with χ estimated from electronic specific heat	Ga	−400	a
	Au	+2300	b
From slope of $\mathcal{K}$ vs χ with temperature an implicit parameter	Ga	−4400	c
	Au	+300 to 600	c
s-band contribution to H_{eff}, assuming $\chi^s_{Pauli} \sim 15\%$ of $\chi(\gamma)$	Ga	12 000 to 14 000	a, d

[a]Assumes the susceptibility is entirely associated with Ga sites (i.e., $\frac{1}{2}\chi$ per Ga site), thus $H^{Ga}_{eff} = N\mu_B \mathcal{K}^{Ga}/W^{Ga}\chi^{AuGa_2}$, with $W^{Ga} = \frac{1}{2}$.

[b]Assumes the susceptibility is entirely associated with the Au site, i.e., $H^{Au}_{eff} = N\mu_B \mathcal{K}^{Au}/\chi^{AuGa_2}$.

[c]Assumes the temperature-dependent change in susceptibility is entirely associated with the site being considered.

[d]See text preceding Eq. (2).

ture-dependent effects are at work.[1] One of these is the turning on of an "s-band" Knight shift. This is required by the T_1 data as tested by the Korringa relation. There remains the question of the nature of the second term, or terms, and the remainder of this section will concentrate on this matter, relying in part on data[18] not available at the time of the orginal Knight-shift paper.

An s-contact-term Knight shift has a much larger hyperfine constant than any competing non-s paramagnetic Knight-shift term. This is suggested by comparison of the free-atom values[5] of the contact term H_s and of the valence p-electron core polarization H_p listed in Table II. We see that the s-hyperfine constant is typically two orders of magnitude larger than p polarization. Granted this, it is probable that the turning on of the s term dominates the temperature dependence of $\mathcal{K}$(Ga), and that the negative term seen at low temperature may either disappear or be present at high temperature. A second temperature-dependent term is then required to explain the susceptibility which becomes increasingly diamagnetic while the paramagnetic s band is turned on. This could arise from the disappearance of paramagnetic terms involving (i) bands of predominantly Au character or (ii) bands of predominantly non-s Ga character, or (iii) increasing band diamagnetism. Jaccarino *et al.* made the second choice, fitting their data with a model involving a Ga p-band term which disappeared with increasing temperature. All three factors are quite possibly important to understanding the susceptibility change.

The energy-band calculations of Switendick and Narath[2] lend credence to the existence of a turned on s-band term while shedding little light on the second effect essential to the susceptibility. One of the conduction bands in these compounds (the "second" band) is of predominantly X-site s character and intersects the Fermi level ϵ_F in $AuAl_2$ and $AuIn_2$ while lying just below it in $AuGa_2$. The calculations indicate that in $AuGa_2$, the second band is quite flat and is ~1 eV below ϵ_F. The authors conclude that this band could be lying much closer to ϵ_F and is thus able to produce Fermi-energy effects at elevated temperatures either by kT smearing or by band shifts associated with lattice expansion or distortion. Strong, but indirect, evidence that simple thermal expansion does not push the $AuGa_2$ second band through the Fermi level was provided by recent de Haas–van Alphen studies[19] indicating that the pressure derivatives of the second band hole sheets of $AuAl_2$ and $AuIn_2$ are positive.

The tendency for the $AuGa_2$ "s band" to lie low is not some idiosyncrasy of the construction of the band potentials. We note that such an effect already appears in the free-atom spectra.[20] The differences in atomic valence s- and p-electron ionization energies are shown in Table III. An atomic valence s electron in Ga lies lowest (~1 eV lower) with respect to the p level of the three atoms Ga, Al, or In. The band calculations have apparently picked up this trend and also the tendency for the s level to lie highest in $AuAl_2$. As noted by Switendick and Narath,[2] the de Haas–van Alphen Fermi-surface data[15] are consistent with these observations in that the second band surface appears to be missing in $AuGa_2$ and the third band surface appears to be smallest in $AuAl_2$. The $AuAl_2$ trend may be associated with the high s position and/or with the absence of low-lying X-site d levels (typically 15 eV below the s and p levels) which hybridize (at least weakly) with the Ga and In bands. The s-p level splittings place these compounds in an order $AuAl_2$-$AuIn_2$-$AuGa_2$. This order is characteristic of some of the existing experimental data and appears in the the Knight-shift temperature dependences of the present paper. It contrasts with the Al-Ga-In order of the Periodic Table which appears to be more appropriate for describing the alloy solubility re-

TABLE II. Free-atom H_s and H_p.

s-electron-contact terms H_s(kOe/μ_B)	p-electron core-polarization terms H_p(kOe/μ_B)[a]
$H_s^{Al} =$ 1 900	$H_p^{Al} = +$ 15
$H_s^{Ga} =$ 6 200	$H_p^{Ga} = -$ 50
$H_s^{In} =$ 10 100	$H_p^{In} = -150$
$H_s^{Au} =$ 20 600	

[a]Based on free-atom P-, As-, and Sb-atom data, the cases for which experimental results exist (see Ref. 5).

TABLE III. Atomic ionization energy (I_A) differences. The s-ionization energy $I_A(s)$ is calculated (Ref. 20) for excitation from the $(^2P)s^2p^1$ ground state to the lowest $(^3P)s^1p^1$ excited multiplet state of the atom. The p involves excitation to the $(^1S)s^2$ state. The Al, In, Ga, Tl order of the energies remains unchanged when comparing neutral atom $s^2p \rightarrow sp^2$ differences.

	$[I_A(s) - I_A(p)]$(eV)
Al	4.7
Ga	6.0
In	5.3
Tl	7.1

sults of the present paper.

As Switendick and Narath point out, their band calculations do not account for the temperature-dependent susceptibility of $AuGa_2$. Before considering the factors which might be dominating the χ behavior, we discuss the s-band susceptibility, which must be overcome by the other terms, but which is responsible for $\mathcal{K}(T)$. Various susceptibility terms are listed in Table IV. The core diamagnetic terms come from Hartree-Fock-Slater calculations.[21] The Pauli susceptibilities $\chi(\gamma)$ are derived from electronic specific-heat γ data,[22] assuming no enhancement effects. The three metals are strongly diamagnetic.

The low-temperature Pauli-paramagnetic terms, as deduced from γ data, are roughly equal for the three compounds with that of $AuGa_2$, some 15% smaller. Assuming that this decrease is a *measure* of the susceptibility χ^s_{Pauli}, of the *missing* s band, one may ask if a term of this scale can be responsible for the high-temperature Knight shift, if it were turned on. As is indicated in Table I, the hyperfine field at the Ga site necessary to make a + 0.5% contribution to $\mathcal{K}^{\text{Ga}}_{\text{tot}}$ (in order to account for its high-temperature value) is 12 000–14 000 kOe/μ_B. This is twice the free-atom s-hyperfine constant (i.e., $\xi = 2$, see Ref. 5) and is not characteristic of a free-electron band which has relatively little s character at its Fermi surface.[5] Such a value is roughly appropriate to a band of purely s character at ϵ_F, as might be obtained in the tight-binding approximation and in the s-like second band as obtained by Switendick and Narath.[2]

Similar calculations for $AuAl_2$ and $AuIn_2$, assuming that 15% of $\chi(\gamma)$ is associated with χ^s_{Pauli}, yield

$$H_s^{\text{Al}} = 1000 \text{ kOe}/\mu_B\,, \quad H_s^{\text{In}} = 16\,000 \text{ kOe}/\mu_B\,. \quad (3)$$

Like Ga, the In value is roughly twice the free-atom value whereas H_s^{Al} is about half. This is consistent with relaxation data[1] which show s-contact terms dominating in $AuIn_2$ and $AuGa_2$ (at high temperatures) but not dominating in $AuAl_2$. In the light of the above observations, one might reasonably conclude that the $AuAl_2$ behavior arises from reduction of s character due to s-p hybridization and/or due to a weaker s-band density of states. These, in turn, are associated with the tendency for the atomic-Al s levels to lie higher relative to the p levels than they do in Ga or In. The ternary alloy results of this paper suggest that the situation is more complicated—In or Ga each have reduced s density similar to the Al when dissolved in $AuAl_2$. The s-p level separation of the host determines the behavior at the impurity site.

It appears that the second or X-site s band is very important to the Knight shift while making but a small contribution, when present, to the density of states at the Fermi level and possibly to most other observables involving states at or near the Fermi surface. The relative importance to the Knight shift arises from s-hyperfine constants which greatly enhance its magnitude. The inflation of the importance of the shift of the second band thus appears to be one essential factor contributing to the AuX_2 anomalies. There remain the questions of the low temperature $\mathcal{K}$ of $AuGa_2$ and of the terms which dominate the temperature dependence of the susceptibility.

JWWM attributed[1] the low-temperature Knight shift to a p-band Fermi surface acting via p "core polarization." Current knowledge of p-electron polarization effects[23] puts this attribution in numerical difficulty (but this knowledge is imperfect). The minimum hyperfine constant necessary to yield the observed low-temperature Knight shift (see Table I) is obtained assuming that the entire low-temperature Pauli susceptibility $\chi(\gamma)$ is associated with Ga-site p bands and it is an order of magnitude larger than atomic p-polarization data (see Table II). The occurrence of negative p-band Knight shifts, which are too large to easily rationalize on the basis of intra-atomic "core-polarization" effects, is not uncommon at p-valence electron sites in various intermetallic compounds.[23] Either p polarization

TABLE IV. Susceptibilities χ in units of 10^{-5} emu/mole.

	Measured[a] χ		Calculated[b] core diamagnetism, assuming Au^+ and two X^t ions.		Pauli $\chi(\gamma)$ (deduced from specific heat γ)[c]
	High temp	Low temp	X^+ions	X^{+3}ions	
$AuAl_2$	− 3.5	− 3.5	− 6.4	−4.2	4.2
$AuGa_2$	− 7.2	− 5.5	− 7.5	−5.5	3.7
$AuIn_2$	−11.7	−11.7	−10.0	−7.6	4.3

[a]Reference 10. [b]Reference 21. [c]Reference 22.

in metals is much stronger than atomic experience suggests, or else other terms are important to the Knight shifts. One such term which appears very attractive for AuX_2 compounds is conduction-electron diamagnetism. These compounds are, after all, diamagnetic, displaying many characteristics of semimetals. There is a suggestion in the data of Table IV that there may be substantial conduction-electron diamagnetism in these compounds. A p-band effective-mass ratio m/m^* of 10 would lead to a Ga-site diamagnetic Knight-shift term[23] of about -0.1% at low temperatures and such effective masses are conceivable. Such diamagnetism could arise from the third and fourth bands or, perhaps, from a fifth band which may produce a small ellipsoid at point K in the Brillouin zone. It is also conceivable that the diamagnetism associated with the turned on s bands makes a substantial contribution to the temperature dependence of the $AuGa_2$ susceptibility, the associated Knight-shift term being swamped by the s-contact interaction. There are hints in the Knight-shift results for the ternary alloys reported in this paper that p core polarization is not completely responsible for the low-temperature Knight shifts.

There are other terms which give negative Knight shifts, such as interatomic effects. In compounds such as $GdAl_2$ or V_3Ga, involving rare-earth or transition-metal atoms, it is quite reasonable to conclude that such magnetic atoms make dominant contributions to the Knight shifts at the less magnetic p-atom sites. The situation at hand is different; the Au sites are presumed to be almost inert, as noted below, and it would be surprising if the local Au-site susceptibility made a substantial contribution to an X-site Knight shift.

The Au as well as the Ga site displays a temperature dependent $\mathcal{K}$ in $AuGa_2$, implying a contribution to $\chi(T)$ as well. Since $d\mathcal{K}/dT$ is negative, it involves either the turning off of a Au s-band contact term or the turning on of $5d$ core polarization. The latter could arise from hybridization with the Ga-site s band but the magnitudes of $d\mathcal{K}/dT$ and of H_d (see Tables I and II) would require something like 50% d hybridization into the Ga band, a situation which seem unreasonable and is inconsistent with the band calculation of Switendick. The alternative of a drop in an s-band term seems more plausible. Given the Au H_s of Table II, the observed change involves a Au-site susceptibility drop which is but 3–6% of the total susceptibility change. In this sense, the Au sites are almost inert with regard to $\chi(T)$. We expect that the Au sites are active with respect to color, and since this has been a matter of some interest, it will be the object considered in Sec. III.

It appears likely that some combination of increasing diamagnetism, decreasing Ga p Pauli term, and decreasing Au-site Pauli term is responsible for the temperature dependence of the susceptibility, with the first and second factors contributing to the low temperature $\mathcal{K}$(Ga) as well. Other than weak Au-site effects, there is no quantitative evidence as to the relative importance of the different contributions. The JWWM model for $AuGa_2$ seems inevitable, except for the minor modification of having several such temperature-dependent terms.

III. Au $5d$ BANDS

It would seem reasonable[10] that the color of Au and Pt intermetallic compounds, such as $AuAl_2$ and $PtGa_2$, is associated with the Au or Pt $5d$ bands. Nevertheless, the original experiments on the AuX_2 compounds were quite successfully interpreted in terms of free-electron bands and this led Vishnubhatla and Jan[11] to conclude that the d bands lie far below ϵ_F and are not responsible for the optical effects. Switendick's band calculations[2] support this view, for they yield Au $5d$-like bands which are ~ 2 eV wide and ~ 7 eV below ϵ_F. We believe that the $5d$ bands are responsible for the colors, with their upper edges lying 3–4 eV below ϵ_F and that soft x-ray photoemission (XPS)[18] and soft x-ray emission (SXS)[24] data of the Au site in $AuAl_2$ indicate this to be so. Of course, whether 7 or 3 eV below ϵ_F, the Au d bands are not directly pertinent to the Fermi-surface effects, which are the main subject of this paper.

The Au-metal[25,26] and $AuAl_2$[18] XPS curves appear in Fig. 1. The optical properties of Au indicate that the Au-metal peak is associated with a $5d$ density of states which has a sharp high-energy edge ~ 2 eV below ϵ_F. A peak and sharp cutoff at the upper edge of the d density of states is characteristic of fcc transition metals. If the d bands of $AuAl_2$ were involved in a similar cutoff, the figure would suggest that they lie 1–3 eV lower than in Au metal with a cutoff 3–5 eV below ϵ_F, depending on which Au spectrum is used and the criteria for the shift. The disparity between the two Au curves of Fig. 1(c) appears to be larger than the disparity between the $4f$-level energies shown in Table V, the latter being a measurement of the calibration difference between the two XPS machines. We believe that the $AuAl_2$ d-band density of states has a much more gradual high-energy edge than in pure Au and that there are hybridized d states 2–4 eV below ϵ_F, the region important to the metal's color.

One may use core-electron-photoemission data to make an independent estimate of the d-band shift. A core- or d-electron energy shift may arise because of a shift in ϵ_F or because the local potential, and hence the one-electron energies, have changed from one metallic environment to another. A shift in ϵ_F of course affects core- and d-electron

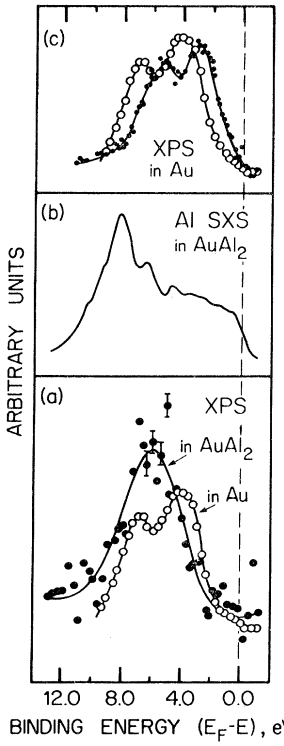

FIG. 1. XPS spectra from the Au 5*d* bands in Au metal (a) and (c), in $AuAl_2$ (a), and SXS spectra from the Al *s* electrons in $AuAl_2$ (b). The Au data in (a) were taken from Fadley and Shirley (Ref. 25) and compared with that of Siegbahn *et al.* (Ref. 26) in (c). The XPS $AuAl_2$ data are that of Chan and Shirley, (Ref. 18) with background subtracted out according to their prescription. The SXS spectrum is from Williams *et al.* (Ref. 33). The curves are shown on a common horizontal energy scale measured with respect to the Fermi level.

positions (with respect to it) equally. The change in local spherical potential due to a charge shift $\Delta\rho$ involving the shift of charge on or off the atomic site in question has a Coulomb energy term

$$\Delta\epsilon_i = \int |\phi_i(r)|^2 (1/r_>)\Delta\rho(r')\,d\tau\,d\tau', \qquad (4)$$

where $r_>$ is the larger of r or r'. A core-electron wave function $\phi_c(r)$ lies entirely inside any normal $\Delta\rho$. As a result, the $1/r_>$ is entirely associated with $\Delta\rho$ and this maximizes $\Delta\epsilon$ for the core electron. Since a *d*-band-electron wave function $\phi_d(r)$ overlaps $\Delta\rho$, its energy is less severely shifted (i.e., it overlaps the shoulder of the potential due to $\Delta\rho$). Core-electron shifts therefore should be as large as, or larger than, the shift of the center of gravity of the *d* bands, providing that the change of environment can be characterized by a simple radial shift of charge on or off the site and by relatively small perturbations of the *d*-band wave function. The experimental positions of the Au 4*f*-shell spin-orbit doublets are tabulated in Table V. We see that these levels lie roughly 1 eV lower[27] in the AuX_2 metals than in pure Au. The $AuAl_2$ data of Fig. 1(a) are consistent with a *d*-band shift of this sort and with a less sharp high-energy cutoff than pure Au. Note that a sharp cutoff in the density of states produces an optical edge, which normally leads to the absorption of all optical energies above the cutoff and reflection below and thus can be responsible for the color of metals and alloys, such as Cu, Au, and the brasses, but cannot produce colors such as the purple of $AuAl_2$. There must be structure in the density of states and/or the transition probabilities associated with the relevant optical energies. The photoemission data suggest that at least the 5*d* bands are in the appropriate energy region. Bands of pure Au 5*d* character, as might be obtained in a band calculation with the *X* sites emptied from the lattice, would be much narrower than what is described above. This width might be as little as 1 or 2 eV. It would seem that an essential feature of *d* bands in transition- or noble-metal compounds is the hybridization with orbitals associated with other types of sites and that this causes a substantial broadening of the density of states involving substantial *d* character. Such effects have been seen, for example, in band calculations[28] for the transition-metal diborides. The situation is similar to *s*-*d* hybridization in the pure transition metals where there tend[29] to be pileups of heavily admixed state densities to one or both sides of the unhybridized *d* density-of-states peak.

The XPS chemical-shift data of Table V would superficially imply a small net charge flow off the Au site. This contrasts with Mössbauer-effect isomer-shift data[30] which have been interpreted as involving a substantial flow of *s*-charge character to the Au site. Taken together, the two sets of experiments indicate[31] strong *s*-*d* charge compensation, i.e., an increase in *s* and decrease in *d* electron count on the Au site in forming the intermetallic compounds.

Soft-x-ray-emission results for Al in $AuAl_2$ are shown in Fig. 1(b). There is a prominent peaking 8 eV below ϵ_F. Switendick[32] believed it to be due to Al hybridization with the Au *d* band and we concur. However, this could either be a marking of the full *d*-band density of states (i.e., Al *s*-band character dragged along by hybridization in the high Au *d*-band peak) or it could simply represent a region of strong Al *s*–Au *d* hybridization at an edge of the *d* peak. We believe that the Al *s* peak does not map the full *d*-band region, which the photoemission data sug-

TABLE V. XPS determination of the 4*f* doublet positions E_{4f} expressed as an energy (eV) below the Fermi energy ϵ_F.

	Upper peak	Lower peak	Ref.
Au	83.75	87.5	a
	84		b
$AuAl_2$	84.5	88.5	c
$AuGa_2$	85.0	88.75	c

[a]As measured from the spectra plotted in Ref. 26, p. 15.
[b]As tabulated in Ref. 25.
[c]As measured from the spectra plotted in Ref. 18.

gest, is broader and lies higher than the Al *s* peak. Note that the Au photoemission peak [Fig. 1(a)] overlaps the energy region of the strong peak of the Al SXS [Fig. 1(b)].[33]

IV. ALLOY PREPARATION AND ANALYSIS

The ternary alloys were prepared from master samples of the binary compounds. The $AuGa_2$ and $AuIn_2$ master samples were made by arc melting weighed amounts of Au and Ga or In in an argon atmosphere while using a titanium getter. The resulting ingots were crushed, and remelted in vacuum-sealed (10^{-6} Torr) quartz ampoules. These were then homogenized at 450 °C for 10 days. The $AuAl_2$ master was made by induction melting in an Al_2O_3 crucible, adding the appropriate amount of Au a little at a time.

The $AuGa_2$-$AuIn_2$ ternary alloys were melted in sealed quartz ampoules using resistance heating. The $AuGa_2$-$AuAl_2$ and the $AuIn_2$-$AuAl_2$ ternary alloys were prepared in an arc furnace and remelted in sealed ampoules in a resistance furnace. All the ternary alloys were homogenized at 450°C for 10 days. The brittle ingots were then crushed to form 200 mesh powder.

X-ray analyses were performed on all of the alloys. X-ray diffraction patterns were made using a diffractometer with Cu target, scanning 2θ at $\frac{1}{2}$ deg/min. Line centers at half-height were taken as line positions. The lattice constants were computer calculated using a least-squares program. For several of the alloys the lines were fairly broad. For the $AuGa_2$-$AuIn_2$ alloys the broader linewidths were not thought to be due to two overlapping lines, since the lines were symmetrical out to high angles without any appearance of an irregularity. Certainly the broad lines may have been due, in part, to the fact that the samples were not annealed after crushing. On the basis of x-ray line broadening, an inhomogeneity in composition of ~ ± 5% was estimated for the $AuGa_2$ + 20 at. % $AuIn_2$ sample, the most concentrated alloy. For the other alloys the inhomogeneity was less.

Pseudobinary solid solution was indicated by x-ray analysis for the ternary alloys of the two systems listed in Table VI. For both systems shown, the change in lattice constant was remarkably linear with composition (Vegard's law), suggesting the possibility of extending the alloying further across these systems, perhaps by a rapid quenching technique such as splat cooling. No extra x-ray lines were seen for the listed alloys.

Metallographic examination using etchants turned out to be inadequate and subsequent metallography was performed on polished unetched surfaces. Whenever a purple phase was present, these regions could be associated directly with the $AuAl_2$-rich phases. The metallographic results were all consistent with x-ray and NMR indications.

In addition, a sample of 1 at. % $AuAl_2$ in $AuGa_2$ was prepared, but its constitution turned out to be less well defined as evidenced by our sample analyses: Although the metallography showed no evidence of second phase, the NMR showed at least two distinct lines of more or less equal intensity in both the ^{27}Al and the ^{69}Ga spectra with one of the ^{69}Ga lines exhibiting a temperature dependence. None of the other alloys showed strong NMR structure at *both* solute and solvent *X* sites. The x-ray lattice constant was also anomalous in that an otherwise monatomic decrease in lattice constant with composition for 0, 2, and 5 at. % $AuAl_2$ in $AuGa_2$ was interrupted by an abrupt decrease for the 1% sample [with measured lattice constant 6.059(2) Å]. The x-ray linewidths were broader for the 1 at. % $AuAl_2$ sample, again indicating anomalous behavior. The x-ray results could be understood by assuming that the 1 at. % nominal composition was erroneous and that there was more than 5 at. % $AuAl_2$. However, this explains neither the existence of the four resonances nor the temperature dependence of one of these. Another possible explanation, which will not be pursued further in this paper, is that for this alloy there is a range of stoichiometry within the AuX_2 phase, in the ternary system Au-Ga-Al.

The extent of alloying for the $AuAl_2$-$AuIn_2$ samples, not listed in Table VI, was determined by the NMR measurements. Qualitatively, second phase was also indicated by metallography and x-ray diffraction. Section V B 3 gives a further discussion of the extent of alloying of $AuAl_2$ with $AuIn_2$ as determined from the observed NMR spectra.

TABLE VI. Room-temperature lattice constants for pseudobinary alloys $AuAl_2$-$AuGa_2$ and $AuGa_2$-$AuIn_2$.

Alloy system	Nominal composition $AuGa_2$ (at.%)	Lattice constant (Å)	Ref.
$AuIn_2$-$AuGa_2$	0 (i.e., $AuIn_2$)	6.517	a, b
	5	6.486(1)	c
	80	6.172(3)	c
	90	6.122(2)	c
	95	6.092(2)	c
	100 (i.e., $AuGa_2$)	6.075	a
$AuAl_2$-$AuGa_2$	98	6.070(3)	c
	95	6.065(2)	c
	5	5.996(2)	c
	0 (i.e., $AuAl_2$)	5.9989	a, d

[a]Lattice constants as given by Pearson (Ref. 34).
[b]Other references report values from 6.50 to 6.53 Å.
[c]C. Bechtoldt (unpublished).
[d]Straumanis and Chopra (Ref. 35) reported that the $AuAl_2$ phase extends from $AuAl_{2.1}$ to $AuAl_{1.95}$ with lattice constant (at 25 °C) varying from 5.9980 to 5.9969, respectively.

V. EXPERIMENTAL METHODS AND RESULTS

A. Methods

Measurements were made using both cw and pulsed NMR. The cw measurements were made at 8 and 16 MHz using a standard commercial nuclear-induction spectrometer with continuous averaging. Most of the reported $\mathcal{K}$ data were measured with the cw equipment.

Pulsed NMR techniques were used to measure T_1 values and to trace out absorption lines in order to verify a few low-temperature Knight-shift values. The spin-echo experiments were performed at 8 MHz with a phase-coherent pulse-coherent crossed-coil spectrometer. The power amplifier was capable of producing an rf field H_1 in the rotating frame, greater than 160 G with rise and fall times less than 0.25 μsec in a transmitter-coil volume of 5 cm^3. Line-shape measurements on the $AuGa_2$-rich alloys containing $AuIn_2$ were carried out at 26 MHz using a smaller power amplifier which produced an H_1 of 40–50 G. For these measurements a superconducting solenoid was employed. Low-temperature measurements were made by inserting the sample and probe into a Dewar containing either liquid helium or liquid nitrogen. The liquid refrigerant was allowed to come into direct contact with the particles of the sample. The effective sample volume was less than 0.5 cm^3. The receiver-detector system had a recovery time of about 15 μsec. Signal-to-noise enhancement was accomplished with a commercial boxcar integrator. Either a saturating comb consisting of 10–20 rf bursts spaced 100 μsec apart or a π pulse was used to saturate or invert the spin-population differences for T_1 measurements. Recovery of the nuclear magnetization was monitored by either the height of an echo produced by two closely spaced $\frac{1}{2}\pi$ pulses or by the amplitude of the free-induction decay following a $\frac{1}{2}\pi$ pulse. In no case was there any indication of failure to saturate the spin system with the H_1 available. Knight-shift and line-shape measurements were made with the pulsed spectrometers by sweeping field and recording the Fourier transform of the free-induction decay or echo using the boxcar integrator. This method yields the full absorption rather than its derivative.[36]

B. Results

1. Knight Shifts

The measured X-site $\mathcal{K}$ values at the various solvent and solute sites in the pseudobinary alloys $AuGa_2$-$AuIn_2$, $AuGa_2$-$AuAl_2$, and $AuAl_2$-$AuIn_2$ are given in Figs. 2–5 and Table VII. All values of $\mathcal{K}$ reported here were obtained by assuming the published room-temperature shift values[1] of 0.056, 0.48, and 0.94% for ^{27}Al in $AuAl_2$, ^{71}Ga in $AuGa_2$, and ^{115}In in $AuIn_2$, respectively. We have attempted to confirm the literature values in the pure intermetallic compounds using $AlCl_3$, $GaCl_3$, and $InClO_3$, as reference salts. Our numbers to match the three quoted above are 0.056, 0.45, and 0.89% for ^{27}Al, ^{69}Ga and, ^{115}In, respectively. Sample preparation or choice of reference salts may account for the small differences and we have not pursued this matter any further.

2. Spin-Lattice Relaxation

The observed spin-lattice relaxation rates $(1/T_1T)$ are summarized in Table VIII. In the $AuGa_2$ alloys, measurements were made on the ^{69}Ga isotope, although T_1 of ^{71}Ga in $AuGa_2$ was measured at 77 °K. Our value of 3.4(1) msec for ^{71}Ga at 77 °K is in good agreement with the T_1 reported previously.[1] The only case where the full linewidth at half-maximum absorption points (~ 500 G at 4.2 °K) exceeded the maximum H_1 available in the rotating frame was ^{115}In in the $(AuGa_2)_{90}(AuIn_2)_{10}$ alloy at 8 MHz. Examination of the recovery of nuclear magnetization following an rf pulse burst consisting of 10–20 equally spaced 2-μsec-wide pulses revealed that at least 70–80% of the ^{115}In nuclear spins were completely saturated. Furthermore, relaxation was characterized by a single exponential term. In light of these observations, it seems reasonable to assume that the T_1 measured in this case is characteristic of the spin system as a whole rather than a fraction of it due to incomplete saturation.[39] At 26 MHz, the ^{69}Ga in $AuGa_2$-$AuIn_2$ alloys exhibited linewidths much larger than the maximum rf field (40 G), but in the few T_1 measurements carried out at this frequency, rf saturation was nearly complete.

A further point to be made is that the measured spin-lattice relaxation rates of ^{69}Ga in this alloy may be influenced by the wings of the ^{115}In resonance which overlap the ^{69}Ga resonance. The

TABLE VII. Temperature-independent Knight shifts of ^{27}Al, ^{115}In, and ^{69}Ga in the nonanomalous alloys. Second phases are not shown but are discussed in the text. The numbers in parentheses represent the estimated error in the last significant figure. Values quoted are for room temperature but those at 77 °K are approximately the same. The errors shown include any temperature dependences between these temperatures.

	^{27}Al $\mathcal{K}$ (%)	^{115}In $\mathcal{K}$ (%)	^{69}Ga $\mathcal{K}$ (%)
$AuAl_2$ + 5 at.% $AuIn_2$	0.056(4)	0.32(2)	···
+95 at.% $AuIn_2$	0.17(5)	0.92(4)	···
$AuGa_2$+95 at.% $AuIn_2$		0.91(4)	0.58(3)
$AuGa_2$ +95 at.% $AuAl_2$	0.056(2)		0.16(2)

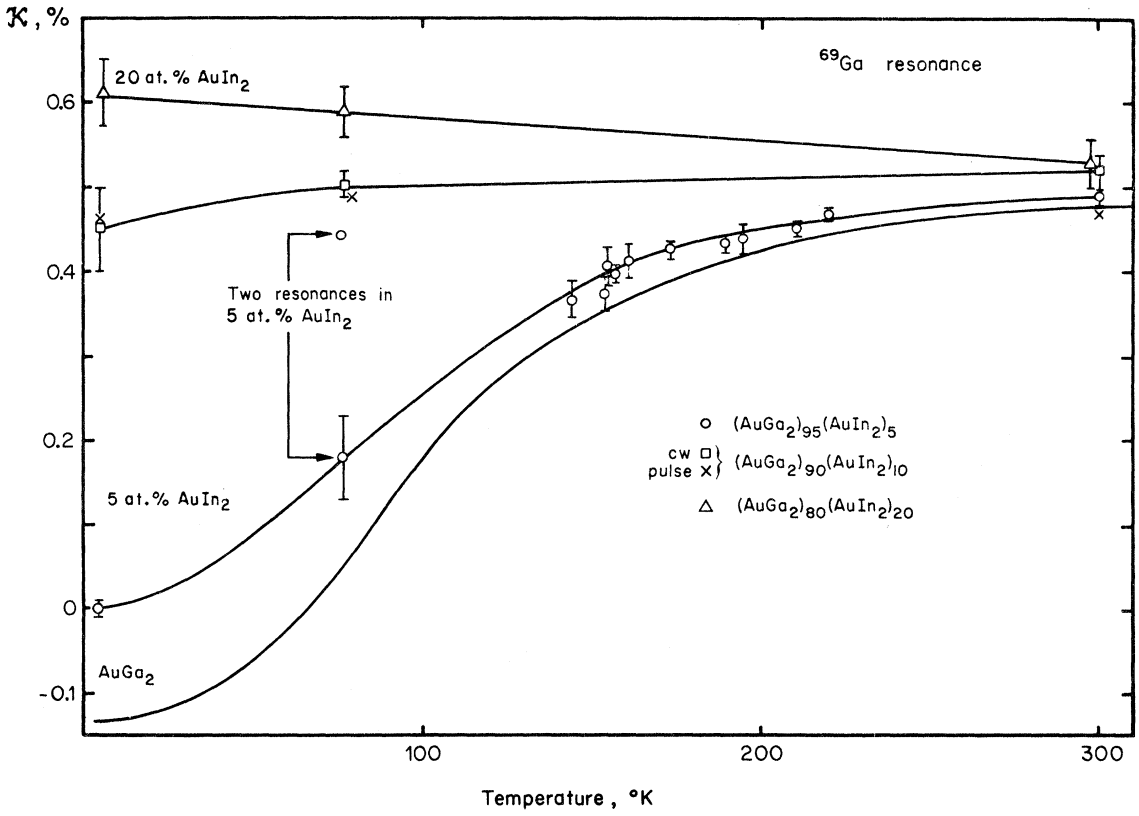

FIG. 2. Temperature dependence of the ^{69}Ga Knight shift in $AuGa_2$-$AuIn_2$ alloys. The $AuGa_2$ line is taken from Jaccarino *et al.* (Ref. 1). The observation of two resonances at 77 °K in the 5 at.% $AuIn_2$ sample is discussed in the text. The lines in this and the other figures (other than that for $AuGa_2$) are drawn for visual ease in viewing the temperature dependences and do not imply any data points in between those explicitly shown.

same could be true of the ^{115}In spin-lattice relaxation time.

From Table VIII it will be noted that the $AuIn_2$ is extremely effective in changing the temperature dependence of the ^{69}Ga relaxation rate in the ternary alloys with respect to pure $AuGa_2$. The rate $(1/T_1T)$ in $AuGa_2$ increases by a factor of 6 in going from 4.2 to 300 °K. Adding only 5% $AuIn_2$ increases the 4.2 °K rate by a factor of almost 4 and the total temperature variation is reduced to less than a factor of 1.8. What is interesting is that the rate remains relatively constant and large at 4.2 °K even though the Knight shift is close to zero. For the ^{69}Ga in the 10% $AuIn_2$ ternary, the 4.2 °K value has increased to ten times the pure $AuGa_2$ rate and almost three times the 5% $AuIn_2$ rate. At 4.2 and 77 °K the increased rates are in accord with the more positive Knight shifts observed in this alloy. These results are also consistent with two or more relaxation mechanisms being operative in these alloys, and with the small negative shift being the result of two terms cancelling, in accord with the JWWM model.

3. *Alloying*

Prior to this work, it was not known whether or not there would be any observable pseudobinary alloying between any two of the three compounds $AuAl_2$, $AuGa_2$, and $AuIn_2$. Evidence that alloying does in fact occur in our alloys is given by x-ray analysis (e.g., Table VI) and metallography, but additional qualitative and quantitative support is available in the NMR data itself. Consider first the room-temperature Knight shifts.

In the $AuAl_2$ matrix, the Knight shift of either ^{69}Ga or ^{115}In is reduced by a factor of about 3 from its room-temperature value in the respective binary compound (see Fig. 4 and Table VII). $\mathcal{K}(^{27}Al)$ is increased by about a factor of 3 for $AuAl_2$ as a solute in $AuGa_2$ or $AuIn_2$ (see Fig. 5 and Table VII). These results verify that some alloying has occurred. An examination of room-temperature Knight shifts is less dramatic for the $AuIn_2$-$AuGa_2$ system, but a continuous smooth variation of the ^{115}In resonance at 300 °K is evident in Fig. 3, suggesting substantial alloying, in agreement with

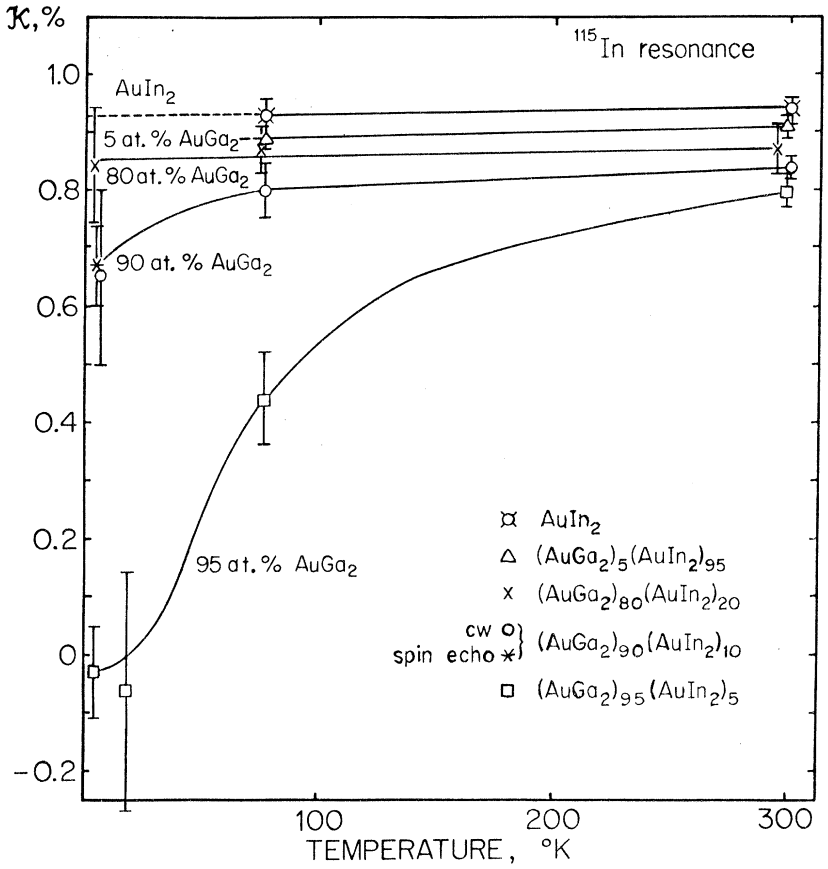

FIG. 3. Temperature dependence of the ^{115}In Knight shift in the $AuGa_2$-$AuIn_2$ system. Only one spin-echo datum point was taken and this is shown as an asterisk. The 77 °K shift in $AuIn_2$ is from this work. The dashed line is extended back to 4.2 °K assuming a constant K as in the literature (Ref. 1).

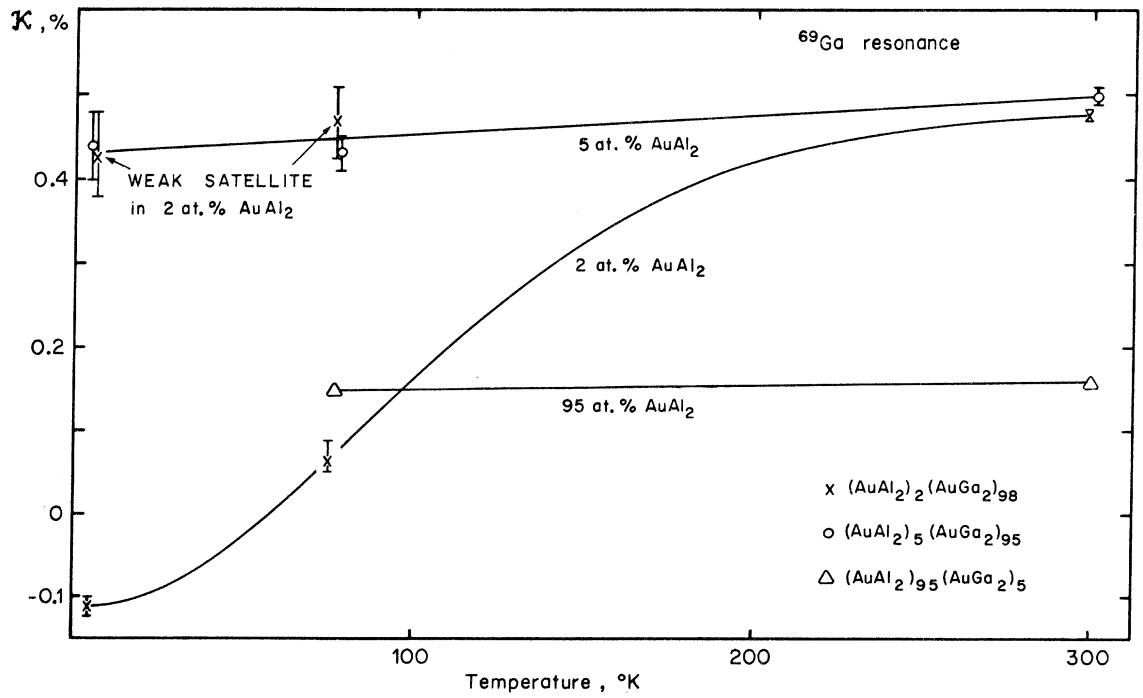

FIG. 4. Temperature dependence of the ^{69}Ga shifts in $AuGa_2$-$AuAl_2$ alloys. Satellite resonances are indicated by the arrows for the 2 at.% alloy and are discussed in the text.

TABLE VIII. Spin-lattice relaxation rates $(1/T_1T)$ in $(\text{sec}\,^\circ\text{K})^{-1}$.

	4.2 °K	77 °K	295 °K	Liquid
		^{69}Ga		
Ga metal				3.3[a,b]
$AuGa_2$	0.82(2)	2.2(1)	5.2(2)	
+ 5 at.% $AuIn_2$	3.3(1)	3.8(1)	5.9(7)	
+10 at.% $AuIn_2$	8.3(2)	7.6(2)	4.5(15)	
+20 at.% $AuIn_2$	8(1)	7(1)		
5 at.% $AuAl_2$		5.2(6)		
		^{27}Al		
Al metal		0.54		
$AuAl_2$		0.050(2)		
+95 at.% $AuGa_2$		0.41(3)		
		^{115}In		
In metal				8.2[a,c]
$AuIn_2$		11.7(2)		
+90 at.% $AuGa_2$	12(2)			

[a]These are the hyperfine-field contributions to the relaxation rate extracted from measurements in the liquid state and expected to be characteristic of free-electron behavior.

[b]Reference 37.

[c]Reference 38.

x-ray diffraction results.

The extent of alloying in the $AuAl_2$-$AuIn_2$ ternary can be deduced quantitatively from the NMR results. Two ^{27}Al NMR lines are observed, for example, in the 95% $AuIn_2$–5% $AuAl_2$ alloy (Fig. 6, top). One of these lines (the low-field line) is shifted substantially from the $AuAl_2$ position, verifying that alloying has occurred. The Knight shift of this line is reported in Table VII. The high-field line is very near to the position of $AuAl_2$ and represents the $AuAl_2$-rich phase. Thus alloying is not complete for 5 at.% $AuAl_2$ in $AuIn_2$. The intensity ratio R of these two lines may be used to estimate the amount of each phase present. We apply the lever rule, modified by the additional fact that the Al concentration is quite different in the two phases. The resulting "enhanced" lever rule[40] exploits the fact that the NMR signal from the less abundant nucleus in a minority phase is enhanced over the ratio of the two phases present, if the nucleus is concentrated in that minority phase. The rule may be written

$$R = I_B(\alpha)/I_B(\beta) = C_\alpha(C_\beta - C)/C_\beta(C - C_\alpha)\,, \qquad (5)$$

where I_B refers to the intensity of the NMR line (estimated for these absorption derivatives by the height multiplied by the square of the width) for nucleus B, in this case ^{27}Al. The α and β refer to the phase boundaries of an $AuIn_2$-rich and an $AuAl_2$-

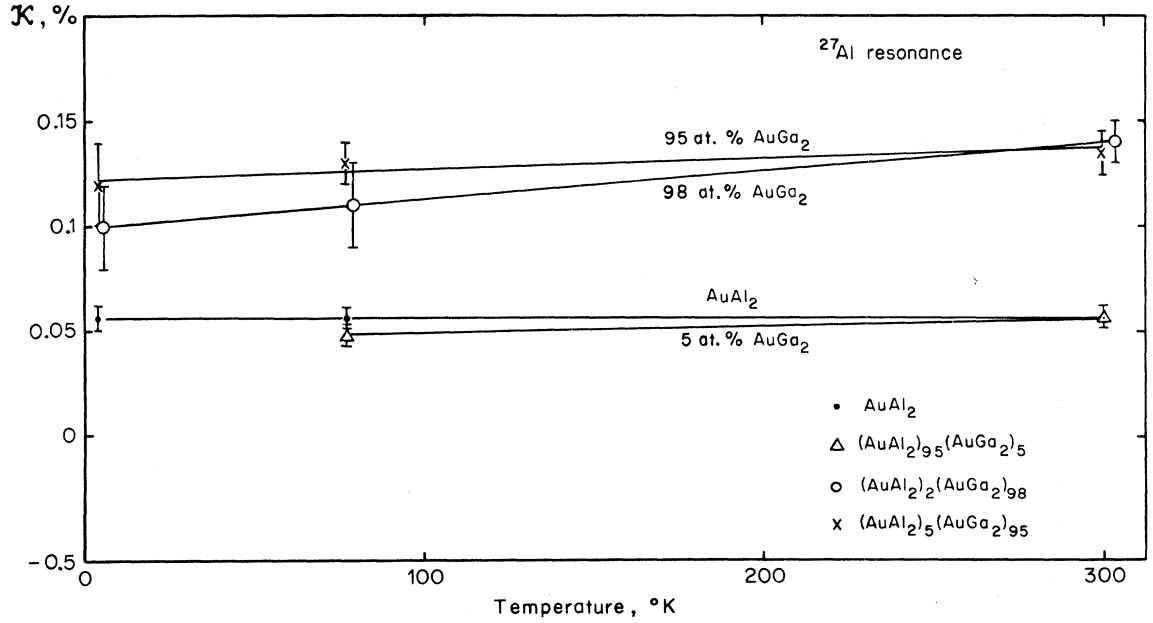

FIG. 5. Temperature dependence of the ^{27}Al Knight shifts in the $AuGa_2$-$AuAl_2$ alloys. Note that the ^{27}Al temperature dependence in $(AuGa_2)_{98}$ $(AuAl_2)_2$ is almost negligible compared with the corresponding ^{69}Ga resonance in this alloy (Fig. 4) and further note that the magnitude of the shift is at least twice that of $AuAl_2$. The $AuAl_2$ data are from this work.

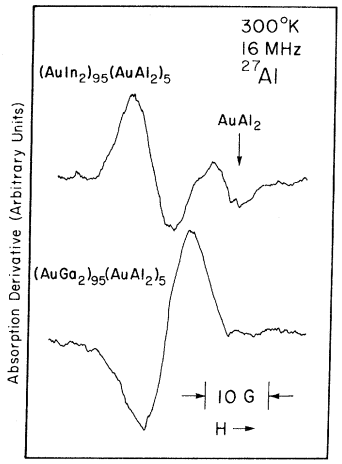

FIG. 6. cw-absorption-derivative spectra obtained for ^{27}Al in a $(AuIn_2)_{95}(AuAl_2)_5$ alloy (top) and in a $(AuGa_2)_{95}(AuAl_2)_5$ alloy (bottom) shown on the same horizontal scale. The data were obtained at 300 °K and at 16 MHz. The magnetic field increases to the right-hand side. The resonance due to the second phase (top) nearly coincides with that of pure $AuAl_2$, shown as an arrow above the trace. It is clear that the $AuAl_2$ has dissolved in the $AuGa_2$ alloy at least to the extent that no second phase is visible above the noise in the lower trace.

rich phase, respectively. The nominal concentration of $AuAl_2$ is $C = 0.05$. The concentration of $AuAl_2$ at α and β is given by C_α and C_β. The formula is not sensitive to the intensity ratio (about 12 in Fig. 6, top) nor to C_β which can be taken, consistent with the metallography and x-ray results, to be about 1 (i.e., 100%), and most important, it implies an enhancement of the Al signal from the Al-rich phase. Thus about 4.5 at.% $AuAl_2$ dissolves in $AuIn_2$, for the metallurgical preparation we have used. This number is not wrong by more than 0.5 at.%, and better precision could be obtained without major effort by estimating C_β and R more precisely.

A similar study of the ^{115}In NMR in $(AuAl_2)_{95}$-$(AuIn_2)_5$ shows that $C_\beta \approx 0.995 \pm 0.003$, or that somewhat less than 1 at.% $AuIn_2$ dissolves in $AuAl_2$. Note that Eq. (5) implies a deenhancement for the majority nuclei, and the second-phase lines are not generally observable for these. Subsequent metallographic analysis gives solubility limits in good agreement with these NMR results. For the $(AuIn_2)_{95}(AuAl_2)_5$ sample the second phase was easily observable because of the bright purple color, quite characteristic of $AuAl_2$, suggesting that no additional intermediate phases exist. The x-ray results indicate the presence of two fluorite phases as well, but do not give accurate quantitative results. Complete solubility of 5 at.% $AuAl_2$ in $AuGa_2$ is confirmed by NMR, as seen in the lower trace of Fig. 6, by the lack of two signals as required by the enhanced lever rule using Eq. (5).

Alloying is also evident in the temperature dependences of the Knight shifts and relaxation times, but this is complicated by the fact that satellite resonances are observed. These satellites are discussed separately in Sec. V B 4.

4. Satellites

NMR is a powerful tool for investigating phase separation as well as microscopic structure in alloys. We have discussed the first of these in Sec. V B 3. In two alloys, $AuGa_2$ + 5 at.% $AuIn_2$ and $AuGa_2$ + 2 at.% $AuAl_2$, where alloying is already confirmed by x-ray diffraction measurements (Table VI and Sec. V B 3), the ^{69}Ga resonance line is asymmetric (see Fig. 7 for the case of $AuGa_2$ + 5 at.% $AuIn_2$ at 77 °K and at 16 MHz). We interpret this asymmetry to be due to a microscopic inhomogeneous Knight shift. In first approximation the spectrum can be decomposed into two lines. The more intense high-field derivative corresponds to the more negative Knight shift (shown in Fig. 2), whereas the broader low-field line is the relatively temperature-independent satellite resonance. At room temperature these two resonances coincide. These lines appear near the resonances of Ga in pure $AuGa_2$ at 77 and 300 °K, respectively. Unlike the origin of the extra Al resonance in the $AuIn_2$ + 5 at.% $AuAl_2$ alloy spectrum shown in Fig. 6, the second resonance here can be established as a satellite arising from microscopic structure rather than as a second-phase signal by the following arguments: (i) X-ray diffraction indicates alloying to be taking place on a large scale in the $AuGa_2$ + 5 at.% $AuIn_2$ alloy and higher $AuIn_2$ concentrations, with no structure other than the fluorite ob-

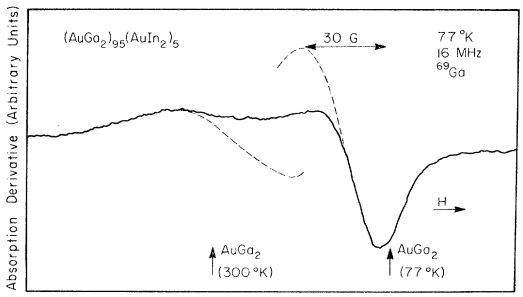

FIG. 7. cw-absorption-derivative spectrum obtained for ^{69}Ga in a $(AuGa_2)_{95}(AuIn_2)_5$ alloy at 77 °K and 16 MHz. The observed spectrum is shown as a solid curve, whereas the two hypothesized components making up the line are shown as dashed curves. These are, respectively, a shifted line (30 G wide) corresponding to Ga with all Ga next-nearest neighbors and a line associated with Ga sites (50 G wide) that have at least one next-nearest In neighbor.

served. (ii) No second ^{115}In resonance is observed in this alloy. If there were even a small amount of phase segregation of a second-phase In-rich fluorite structure, then the enhanced lever rule [Eq. (5)] would lead to a relatively strong ^{115}In line with a $\mathcal{K}$ characteristic of the pure $AuIn_2$. No such line appears. It is clear from Fig. 3 that the $\mathcal{K}$ of the ^{115}In in $AuIn_2$ is quite separated from the 77 °K value of the observed line in the $AuGa_2$ + 5 at.% $AuIn_2$ alloy so that the second-phase In resonance line would not overlap the observed In resonance and thus should be easily observable. It will be recalled that in the case of $AuIn_2$ + 5 at.% $AuAl_2$ (Fig. 6) the second ^{27}Al resonance not only appears but has the intensity enhancement relative to the ^{27}Al signal in the dissolved Al phase, expected from the enhanced lever rule. (iii) The systematic increases in the ^{69}Ga relaxation rate (at 77 °K and below) and in $\mathcal{K}$ at the principal ^{69}Ga and ^{115}In sites with the addition of $AuIn_2$ to $AuGa_2$, at any given temperature, is consistent with alloying. The low temperature for ^{115}In (in 5 at.% $AuIn_2$) is more characteristic of a $AuGa_2$ than a $AuIn_2$ matrix, and its temperature dependence tracks that of the Ga shift. There exists systematic poisoning of the temperature dependence at both sites with increasing $AuIn_2$ concentration. These all suggest that a second metallurgical phase which might account for the observed satellite is unlikely. (iv) The modified lever rule [Eq. (5)] applied to the Ga site in the Ga-rich alloys leads to a signal deenhancement of any second line to an extent inconsistent with the observed second peak in Fig. 7 or 8.

A similar but weaker resonance satellite appears in the ^{69}Ga spectrum of the $AuGa_2$ + 2 at.% $AuAl_2$ alloy at 77 °K, as indicated in Fig. 4. In this case the ^{27}Al solute resonance is shifted to a much different value than in $AuAl_2$ and, unlike the In case, is relatively temperature independent. Again x-ray diffraction measurements show no second phase and no second ^{27}Al resonance is observed which should be expected from the enhanced lever principle. Therefore, as in the In case, the satellite must arise from microscopic structure in the alloyed phase rather than from a precipitated second phase.

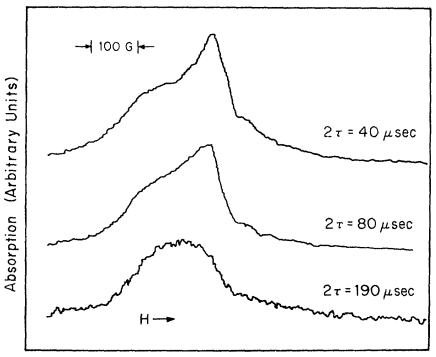

FIG. 8. Absorption spectra obtained at 4.2 °K and 26 MHz by Fourier transforming the spin echo of ^{69}Ga in $(AuGa_2)_{95}$-$(AuIn_2)_5$ as a function of magnetic field. The line shapes are shown for three different pulse-separation times τ. (The echo appears in the vicinity of 2τ.) The magnitude of the rf field is 30–40 G and the echo was found to maximize with two equal width 4–5-μsec pulses. The intensities of the three lines are not calibrated with respect to one another.

The satellites are due to local environments. In all but the most dilute alloys, such Knight-shift satellites normally manifest themselves only as line broadening. We believe that the observation of an at least partially resolved satellite, encountered here at relatively high concentrations, is due to the nature of the X-site environment. The X site's nearest neighbors are Au atoms which are not replaced upon alloying; alloying instead involves X-type atoms at second-, third-, and more-distant-neighbor sites. In some sense, the screening by the Au causes the system to act like a "dilute" alloy. A similar case of NMR satellite observation in a pseudobinary alloy system was encountered[41] for ^{59}Co in $(TiFe)_x(TiCo)_{1-x}$, and had a similar origin.

In order to elucidate the line-shape mechanism in the $AuGa_2$ + 5 at.% $AuIn_2$ alloy, the spin-echo signal from the ^{69}Ga was Fourier transformed by sweeping field at 26 MHz and 4.2 °K. The full absorption spectra thus obtained are exhibited in Fig. 8. It is apparent that there are at least two different lines, in agreement with the interpretation of the cw derivative lines shown in Fig. 7.

The broad line at $2\tau = 190$ μsec, which corresponds to the temperature-independent resonance in the cw spectrum (Figs. 2 and 7), appears to have a longer transverse decay time T_2 than the narrower peak observed at $2\tau = 40$ μsec. The shift on the latter matches that of the more intense derivative in Fig. 7 and, in turn, corresponds to the strongly temperature-dependent Ga line in Fig. 2. An unambiguous separation of the two component resonances is not possible in either Fig. 7 or 8 because one or both components are asymmetric arising perhaps from other unresolved satellite or quadrupolar structure. Nevertheless, a partial decomposition of the resonance into two components is shown in Fig. 7. It is clear that the two components do not add up exactly to the observed spectrum, but they do give a qualitative picture of most of the line structure. For small amounts of asymmetry, the crossover point of each component is found to be relatively insensitive to line shape. While the data for Fig. 7 are taken at 77 °K, the pulsed NMR data of Fig. 8 are recorded at 4.2 °K.

Comparison of the line profile with those obtained at 8 MHz confirm that the lines are inhomogeneously

magnetically broadened. Anisotropic Knight shift in a cubic structure can be ruled out on the grounds that in a powdered random alloy a symmetric shape would be expected.[42] There is also the possibility (though not probable) of a crystallographic transformation to a noncubic structure in the alloy at low temperatures. An anisotropic Knight-shift powder pattern could then appear.

We searched for separate spin-lattice relaxation rates by centering the magnetic field at the different resonance peak positions. The sharp peak yielded a rate in agreement with the 8-MHz results, whereas the broad peak at $2\tau = 190$ μsec seemed characterized by a rate which was about 30% faster than the number shown in Table VIII. However, the signal-to-noise ratio and rf saturation were not sufficiently strong to make this statement with any certainty.

VI. DISCUSSION

We have observed a complicated array of Knight-shift and relaxation-time behavior which at times is temperature dependent and at other times not, and which at times reflects the alloy host characteristics and at other times does not. In order to discuss these effects, we will, as is often done,[5,43] try to characterize the behavior of an alloy system as "local" versus "nonlocal" or "bandlike" in nature. By local we mean that the properties of a single site and its immediate environment determine the behavior at that site, and by nonlocal we mean that a substantial region in the alloy is important to the behavior at the single site. No clear choice can be made for the AuX_2 alloy data. Let us first consider the implication of the temperature dependent $\mathcal{K}$'s.

The ^{69}Ga resonance is temperature dependent in the more Ga-rich alloys. The introduction of either $AuIn_2$ or $AuAl_2$ eventually poisons the $AuGa_2$ temperature dependence. $AuAl_2$ is the more efficient poisoner and this is probably associated with the s-p level differences seen in Table III and may be related to the lower solubility of $AuAl_2$ in $AuGa_2$. It is interesting that the ^{69}Ga and ^{115}In resonances display a common temperature dependence in the $AuGa_2$-$AuIn_2$ alloys. The extent that this is so can be seen by comparison of Figs. 2 and 3 or by inspection of Fig. 9, and this is consistent with the "band" description for this alloy system. Note that the introduction of In does cause a change in the ^{69}Ga temperature dependence. The ^{27}Al resonance position in the $(AuGa_2)_{98}$-$(AuAl_2)_2$ alloy, on the other hand, displays relatively little temperature dependence while that for ^{69}Ga varies significantly. It is, of course, possible that there might be an ^{27}Al temperature dependence at lower Al concentrations, but in any case, it appears that the Al is sufficiently different from the Ga site so as to not be dragged along as strongly as In by Ga s-band effects. The band trend for $AuIn_2$ and apparently local trend for $AuAl_2$ as solutes in the $AuGa_2$ matrix is quite consistent with the fact that the X-site s band lies lowest, relative to the p band, in $AuGa_2$ and highest in $AuAl_2$.

There is evidence of local behavior even in the $AuGa_2$-$AuIn_2$ system, which, as we have just noted, displays a semblance of band effects. For example, the presence of a temperature-independent satellite together with a temperature-dependent shift at the Ga site in the $AuGa_2$ + 5 at.% $AuIn_2$ alloy is due to a local poisoning of the Ga resonance by In neighbors. The intensity of the satellite is about equal to that of the principal line. For random distribution, roughly one fourth of the Ga sites have at least one In atom on the nearest-six X-neighbor sites. Thus the poisoning effect necessarily involves the nearest-18 X-site neighbors. A model in which poisoning occurs for one or more In on any of these 18 sites would imply a satellite intensity larger than measured. A more complicated model or nonrandomness might account for this discrepancy.

It is distinctly odd that the ^{115}In resonance tracks the ^{69}Ga temperature-dependent shift while presumably poisoning the temperature dependence of its Ga near neighbors. While no simple explanation seems available for this oddity, the presence of the satellite suggests the importance of local effects. The temperature-independent ^{69}Ga satellite in the 2 at. % $AuGa_2$-$AuAl_2$ systems (see Fig. 4) is again consistent with a model in which an impurity poisons the temperature variation of the Ga sites in its immediate vicinity. Unlike In, the poisoning Al site displays a temperature-independent shift.

The high-temperature Knight shifts suggest that the alloy host dominates in determining X-site Knight-shift behavior. The high-, rather than the low-temperature shifts, are appropriate for com-

TABLE IX. Normalized solute X-site Knight shifts $\mathcal{K}(AuX_2)$ in the host AuY_2 at 300 °K, as ascertained in three ways: $\mathcal{K}^{\text{solute}}/\mathcal{K}(X \text{ in } X \text{ metal})$, $\mathcal{K}^{\text{solute}}/\mathcal{K}(X \text{ in Au host})$, and $\mathcal{K}^{\text{solute}}/H_s^{\text{atom}}(X)$ (scaled). $H_s^{\text{atom}}(X)$ is taken from Table II. The scaling is chosen to set the value for ^{115}In in $AuIn_2$ equal to 1.1.

Host AuY_2 \ Solute AuX_2	$AuAl_2$ ^{27}Al	$AuGa_2$ ^{69}Ga	$AuIn_2$ ^{115}In
$AuAl_2$	0.35	0.36	0.39
	0.33	0.23	0.37
	0.35	0.30	0.35
$AuGa_2$	0.84	1.1	0.98
	0.79	0.70	0.93
	0.81	0.91	0.94
$AuIn_2$	1.1	1.3	1.1
	1.0	0.84	1.1
	1.1	1.1	1.1

parison since presumably the $AuGa_2$ s band participates at high temperatures. Normalized shifts are listed in Table IX. Three methods of normalization are employed so as to separate real trends from the idiosyncrasies of a particular normalization scheme. The alloy shifts have been normalized (i) with respect to the $\mathcal{K}$ of pure Al, Ga, and In metals; (ii) with respect to the shifts for these atoms as dilute impurities in Au metal; and (iii) by dividing by the H_s of Table II. Since (iii) normalizes the ratios in a different manner than (i) or (ii), we have arbitrarily scaled it, so that the value for In in $AuIn_2$ matches the values from the other two schemes. The three normalizations yield essentially identical Al and In results with a somewhat greater scatter for Ga. Pure-Ga metal has an anomalous band structure and $\mathcal{K}$, and the scatter may be associated with this tendency. The normalized $\mathcal{K}$ are seen to be essentially identical for any X in a given host and are markedly smaller when that host is $AuAl_2$. It is notable that Al in $AuGa_2$ conforms to the pattern while not tracking the $AuGa_2$ temperature dependence. The smaller value for $AuAl_2$ is most easily rationalized in terms of a reduced s-band susceptibility in that compound, but there is no hint of such a tendency in either χ or the specific heat γ (see

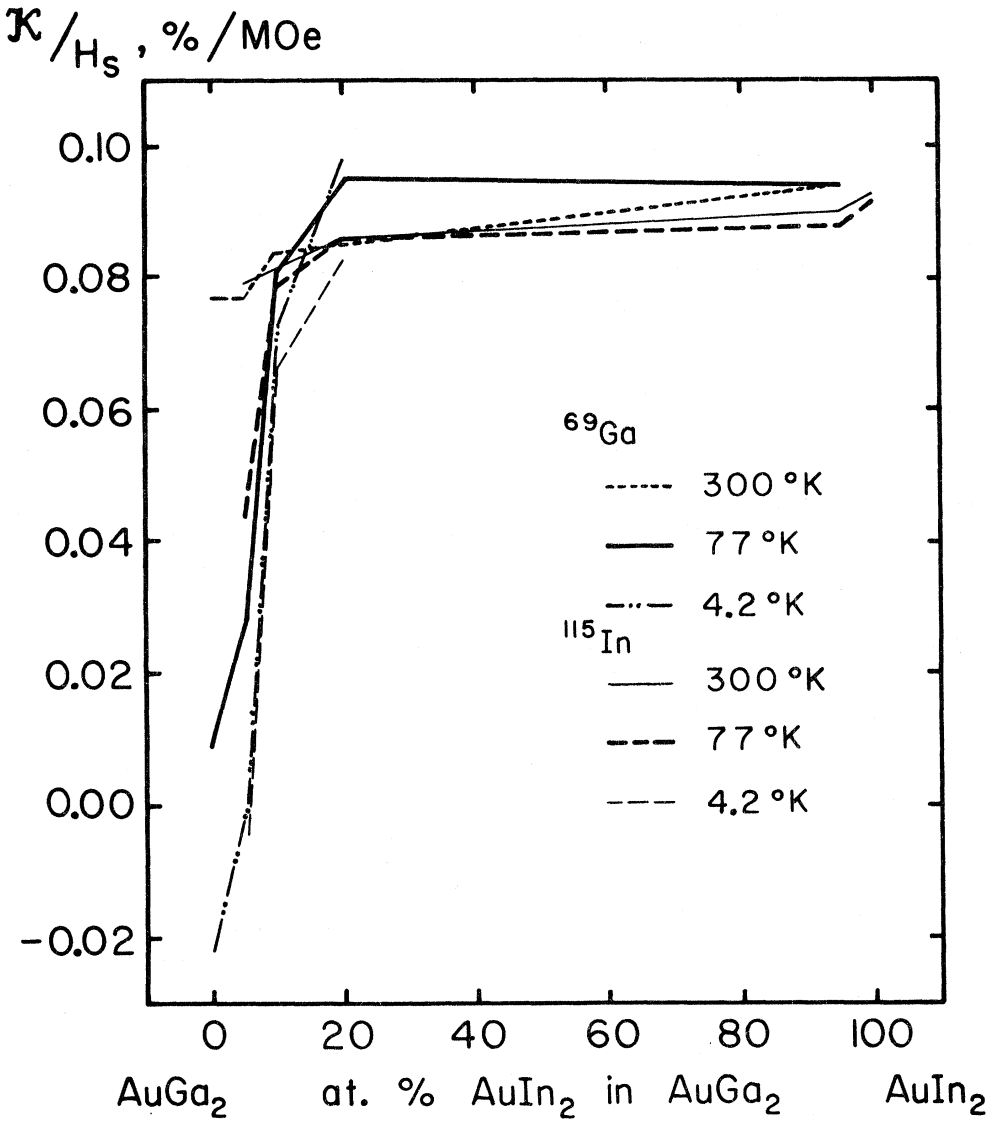

FIG. 9. Normalized shifts of ^{69}Ga and ^{115}In vs $AuIn_2$ concentration in the $AuGa_2$-$AuIn_2$ system at three temperatures. The shifts are normalized by dividing by the s-hyperfine field H_s^i of the respective nucleus i in order to give a measure of the s character. Lines are drawn to connect the data points for the concentrations 0, 5, 10, 20, and 95 at.% $AuIn_2$ in $AuGa_2$. Satellite resonances are excluded from this figure.

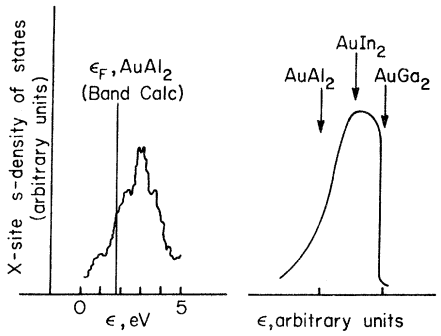

FIG. 10. Plot of the s density of states as a function of energy measured with respect to the Fermi level in AuX_2 compounds (X=Al, In, and Ga). The left-hand side shows the Al s density of states in $AuAl_2$ calculated by Switendick (Ref. 32). The right-hand side schematically shows a possible location of the Fermi levels in $AuAl_2$, $AuIn_2$, and $AuGa_2$, respectively.

Table IV). We might note that the relaxation times, taken with the $\mathcal{K}$, indicate that s-band effects are weaker in $AuAl_2$ than the other two compounds. There is a suggestion of such an s reduction in Switendick's band results.[32] Plotted in Fig. 10 is Switendick's Al s-orbital contribution to the density of states of $AuAl_2$ in the vicinity of ϵ_F. We shall assume that the peak is predominantly due to structure in the s band though, of course, there will be some contributions from hybridization with other bands. We see that ϵ_F falls low in the peak, implying a smaller s-band Pauli susceptibility than if it intersected the maximum. ϵ_F is expected to fall higher in the peak in $AuIn_2$, since the In atomic-s level, and hence the s band, lies lower with respect to the p band. The s level lies still lower in $AuGa_2$ and, consistent with the JWWM model, ϵ_F can be expected to fall just above the s peak. This trend is illustrated schematically on the right-hand side of Fig. 10. The high-energy edge of the band has been drawn more sharply than the $AuAl_2$ result. This is consistent with the band results to the extent that the s bands are flatter in $AuGa_2$, which is necessary if the $AuGa_2$ s band is to be "turned on" with temperature. The situation is unusual in that strong density-of-states structure, of the sort producing temperature-dependent Fermi-surface effects, is normally considered characteristic of d and not s or p bands.

The relaxation times provide further evidence supporting a nonlocal model of alloy effects. Korringa products $\gamma^2\mathcal{K}^2T_1T$ are listed in Table X and are of interest in the few cases where data were obtained for both X sites at some given temperature. The products, like the normalized $\mathcal{K}$'s, are essentially identical for a given alloy.

The present alloy Knight-shift temperature dependences are consistent with the Al-In-Ga order indicated by the atomic s-p splittings and the band calculations, and are suggested by some of the experimental data reviewed in Sec. II. Instead, the alloy solubilities follow the Periodic Table order. The $AuAl_2$-$AuIn_2$ system has the narrowest range of solubility. This may be due to atomic size predominating over band effects. The s-p level splittings listed in Table III suggest that it might be useful to attempt (we have not) to alloy Tl into the X site of $AuGa_2$, or if need be, another of the compounds as a further test of the s-band model. The atomic s level in Tl lies even lower, relative to the p level, than in Ga. One would thus expect a tendency towards diamagnetic temperature-independent $\mathcal{K}$ characteristic of $AuGa_2$ at low temperatures.

The alloying effects encountered here are consistent with the band calculations and thus in some limited sense provide corroboration for the model proposed by Jaccarino and co-workers.[1] Neither the present results nor the band calculations provide insight into the second term, or terms, contributing to the $AuGa_2$ temperature-dependent susceptibility. They only indicate the likelihood of a temperature-dependent s-band effect, not present in the other two compounds, which seems to be associated with the atomic s-p splitting. The alloy results introduce some complications of their own. If it were not for the presence of satellites and the temperature-independent Al resonance in $(AuGa_2)_{98}$-$(AuAl_2)_2$, the alloys would readily be described in terms of a nonlocal model. The satellites suggest

TABLE X. Experimental Korringa products ($\pi k\hbar\gamma^2\mathcal{K}^2T_1T\mu_B^{-2}$).

	4.2 °K	77 °K	295 °K
	^{69}Ga		
$AuGa_2$	0.50(1)	0.02(1)	1.0(1)
+ 5 at.% $AuIn_2$	<0.001	0.2(1)	0.9(1)
+10 at.% $AuIn_2$	0.5(2)	0.7(1)	1.3(4)
+20 at.% $AuIn_2$	1.0(3)	1.1(3)	
+ 5 at.% $AuAl_2$		0.8(2)	
	^{27}Al		
$AuAl_2$		1.5(4)	
+95 at.% $AuGa_2$		1.0(3)	
	^{115}In		
$AuIn_2$		1.3(1)	
+90 at.% $AuGa_2$	0.7(2)		

the presence of far more local effects. As we have indicated, the satellites are a property of the alloys and not of second phases in the samples. As such, they must be taken seriously. The result is an amalgam of local and nonlocal effects which are not obviously consistent with one another. The Au *d* bands are playing little or no role in the effects concerning us here but, contrary to the conclusions of some of the previous workers (see Sec. III), we believe the *d* bands are at least responsible for the fact that $AuAl_2$ is purple.

ACKNOWLEDGMENTS

We thank C. Bechtoldt for x-ray diffraction measurements, D. P. Fickle for sample preparation, C. Brady for metallographic examination, and R. L. Parke for aid with the measurements. We have benefited from conversations with A. Narath, D. Shirley, A. Switendick, L. J. Swartzenruber, and J. H. Wernick. We thank M. L. Perlman and J. Hudis for XPS measurements and useful discussions.

---

*Also Consultant, National Bureau of Standards, Gaithersburg, Md.

†Work supported by the U. S. Atomic Energy Commission.

[1]V. Jaccarino, M. Weger, J. H. Wernick, and A. Menth, Phys. Rev. Letters 21, 1811 (1968).

[2]A. C. Switendick and A. Narath, Phys. Rev. Letters 22, 1423 (1969).

[3]J. P. Jan and W. B. Pearson, Phil. Mag. 8, 279 (1963).

[4]J. T. Longo, P. A. Schroeder, and D. J. Sellmyer, Phys. Letters 25A, 747 (1967).

[5]L. H. Bennett, R. E. Watson, and G. C. Carter, J. Res. Natl. Bur. Std. (U.S) 74A, 569 (1970).

[6]K. C. Brog and W. H. Jones, Jr., Phys. Rev. Letters 24, 58 (1970).

[7]A. Narath, K. C. Brog, and W. H. Jones, Jr., Phys. Rev. B 2, 2618 (1970).

[8]A. Narath and A. C. Gossard, Phys. Rev. 183, 391 (1969); A. Narath (private communication).

[9]L. Pauling, *The Nature of the Chemical Bond* (Cornell U.P., Ithaca, N.Y., 1960).

[10]J. H. Wernick, A. Menth, T. H. Geballe, G. Hull, and J. P. Maita, J. Phys. Chem. Solids 30, 1949 (1969).

[11]S. S. Vishnubhatla and J. P. Jan, Phil. Mag. 16, 45 (1967).

[12]Note, however, that the atomic radius is not a wholly satisfactory parameter in alloy theory [see, e.g., T. B. Massalski and H. W. King, Progr. Mater. Sci. 10, 1 (1963)]. N. F. Mott [Acta Cryst. 13, 980 (1960)] has argued that the volume associated with an atom is of greater significance to an understanding of the nature of the chemical bonding. The volume of an AuX_2 molecule in the compound is larger than that of the constituent atomic volumes by about 7% for $AuAl_2$ and by 1–2% for $AuGa_2$ and $AuIn_2$. The volume change in $AuAl_2$ implies a substantial lowering (estimated $\sim \frac{1}{2}$ eV) in the position of the Au 5*d* band (see Ref. 31).

[13]L. H. Bennett, R. W. Mebs, and R. E. Watson, Phys. Rev. 171, 611 (1968).

[14]A. R. Storm, J. H. Wernick, and A. Jayaramon, J. Phys. Chem. Solids 27, 1227 (1966).

[15]J. P. Jan, W. B. Pearson, Y. Saito, M. Springford, and I. M. Templeton, Phil. Mag. 12, 1271 (1965).

[16]V. Jaccarino, W. E. Blumberg, and J. H. Wernick, Bull. Am. Phys. Soc. 6, 104 (1961).

[17]A. M. Clogston and V. Jaccarino, Phys. Rev. 121, 1357 (1961).

[18]P. D. Chan and D. A. Shirley, in *Electronic Density of States*, edited by L. H. Bennett, Natl. Bur. Std. Spec. Publ. 323 (U.S. GPO, Washington, D.C., 1972).

[19]J. E. Schirber and A. C. Switendick, Solid State Commun. 8, 1383 (1970).

[20]C. E. Moore, Natl. Bur. Std. (U.S.) Circ. 467 (U.S. GPO, Washington, D.C., 1949).

[21]C. M. Hurd and P. Coodin, J. Phys. Chem. Solids 28, 523 (1967).

[22]J. A. Rayne, Phys. Letters 7, 114 (1963).

[23]R. E. Watson, L. H. Bennett, G. C. Carter, and I. D. Weisman, Phys. Rev. B 1, 222 (1971).

[24]A. J. McAlister, J. R. Cuthill, R. C. Dobbyn, and M. L. Williams, in *Proceedings of the Second International Conference on Band-Structure Spectroscopy of Metals and Alloys, Strathclyde, Glasgow, Scotland*, edited by D. J. Fabian (Academic, New York, to be published).

[25]C. S. Fadley and D. A. Shirley, J. Res. Natl. Bur. Std. (U.S) 74A, 543 (1970).

[26]K. Siegbahn, C. Nordling, A. Fahlman, R. Nordberg, K. Hamrin, J. Hedman, G. Johansson, T. Bergmark, S-E. Karlsson, I. Lindgren, and B. Lindberg, *ESCA Atomic, Molecular and Solid State Studied by Means of Electron Spectroscopy* (Almqvist & Wiksells, Uppsala, 1967).

[27]There are obvious questions of calibration errors when considering chemical shifts this small. More recent measurements made specifically to minimize calibrating errors (see Ref. 31) indicate that the 1-eV shift is indeed characteristic of the chemical shift, relative to ϵ_F, in going from Au to AuX_2.

[28]A. J. McAlister (private communication).

[29]See, for example, L. Hodges, H. Ehrenreich, and N. D. Lang, Phys. Rev. 152, 505 (1966).

[30]P. H. Barrett, R. W. Grant, M. Kaplan, D. A. Keller, and D. A. Shirley, J. Chem. Phys. 39, 1035 (1963).

[31]R. E. Watson, J. Hudis, and M. L. Perlman, Phys. Rev. (to be published).

[32]A. C. Switendick, in *Electronic Density of States*, edited by L. H. Bennett, Natl. Bur. Std. Spec. Publ. 323 (U.S. GPO, Washington, D.C., 1971).

[33]M. L. Williams, R. C. Dobbyn, J. R. Cuthill, and A. J. McAlister, in *Electronic Density of States*, edited by L. H. Bennett, Natl. Bur. Std. Spec. Publ. 323 (U.S. GPO, Washington, D.C., 1971).

[34]W. B. Pearson, *Handbook of Lattice Spacings and Structures of Metals* (Pergamon, New York, 1967), Vol. 2.

[35]M. E. Straumanis and K. S. Chopra, Z. Physik. Chem. (Frankfurt) 42, 344 (1964).

[36]W. G. Clark, Rev. Sci. Instr. 35, 316 (1964).

[37]D. A. Cornell, Phys. Rev. 153, 208 (1967).

[38]F. Rossini, E. Geissler, E. M. Dickson, and W. D.

Knight, Advan. Phys. 16, 287 (1967).
[39]W. W. Simmons, W. J. O'Sullivan, and W. A. Robinson, Phys. Rev. 127, 1168 (1962).
[40]L. H. Bennett and G. C. Carter, Met. Trans. 2, 3079 (1971).
[41]L. J. Swartzendruber and L. H. Bennett, J. Appl. Phys. 39, 2215 (1968).
[42]R. J. Snodgrass and L. H. Bennett, Phys. Rev. 132, 1465 (1963).
[43]W. D. Knight, *Solid State Physics*, edited by F. Seitz and D. Turnbull (Academic, New York, 1956), Vol. 2, p. 93.

PHYSICAL REVIEW B VOLUME 5, NUMBER 9 1 MAY 1972

Formulation of the Constant-Coupling Approximation

H. Falk
Department of Physics, City College of the City University of New York, New York, New York 10031
(Received 17 September 1971)

We utilize a Glauber identity to formulate the $S=\frac{1}{2}$ Ising-model problem. This formulation provides a concise view of some connections between the molecular field and the constant-coupling approaches and may provide a useful medium for generating and testing other approximations.

I. INTRODUCTION

The constant-coupling approximation, introduced by Kasteleijn and van Kranendonk,[1-4] provides a method for calculating equilibrium properties of spin systems. The method attempts to deal with correlations which the usual molecular field approximations neglect, and some results of the constant-coupling approximation, e.g., critical-temperature values, represent an improvement over molecular field results.

To gain broader understanding of the constant-coupling approximation seems a worthwhile goal, since the approximation is related to the important general problem[5] of obtaining reliable reduced statistical operators for many-particle systems. It is noteworthy that the constant-coupling approximation is applied to the two-spin reduced statistical operator which has inherited its structure from the exact N-spin statistical operator, whereas the molecular field method hinges on a variational technique[6] in which a *trial* N-spin statistical operator is written as a product of one-spin operators.

In addition to the original work of Kasteleijn and van Kranendonk, general cluster expansions[7] for Heisenberg and Ising systems have been shown to provide a common framework for arriving at both the molecular field and constant-coupling approximations; however, the cluster expansions tend to be rather complicated and do not seem the most efficient route toward the particular goal stated above.

With that in mind we discuss the formulation of the $S=\frac{1}{2}$ Ising-ferromagnet problem in terms of a spin probability identity[8] which Glauber presented. The formulation provides a relatively concise view of some connections between the molecular field and the constant-coupling approaches and may provide a useful medium for generating and testing other approximations.

II. MARGINAL SPIN PROBABILITY

In this section we develop some techniques which are model independent insofar as they apply to any collection of spins of magnitude $\frac{1}{2}$ irrespective of the Hamiltonian or ensemble.

Consider a system of N spins, each of magnitude $\frac{1}{2}$, and let s_i denote the operator for the z projection of the ith spin:

$$s_i = \pm 1, \quad i = 1, 2, \ldots, N . \tag{2.1}$$

Of the 2^N spin configurations, focus attention on those with a particular value of

$$m = (1/N) \textstyle\sum_i s_i \tag{2.2}$$

and let $\langle \cdots ; m \rangle_N$ denote a conditional average over the set M of spin states with the same m. Now we utilize the Glauber[8] identity to write the exact two-spin conditional probability in the implicit form

$$p_N(s_i, s_j; m) = \tfrac{1}{4}(1 + \langle s_i ; m\rangle_N s_i + \langle s_j ; m\rangle_N s_j + \langle s_i s_j ; m\rangle_N s_i s_j) , \tag{2.3}$$

where $1 \leq i < j \leq N$.

For a homogeneous system

$$m = \langle s_i ; m\rangle_N, \quad i = 1, 2, \ldots, N \tag{2.4}$$

so that

$$p_N(s_i, s_j; m) = \tfrac{1}{4}[1 + (s_i + s_j)m + s_i s_j \langle s_i s_j ; m\rangle_N] . \tag{2.5}$$